PHYSICAL REVIEW LETTERS **125,** 023002 (2020)

Editors' Suggestion Featured in Physics

Laser Resonance Chromatography of Superheavy Elements

Mustapha Laatiaoui,[1,2,3,4,*] Alexei A. Buchachenko,[5,6] and Larry A. Viehland[7]
[1]*Department Chemie, Johannes Gutenberg-Universität, Fritz-Strassmann Weg 2, 55128 Mainz, Germany*
[2]*Helmholtz-Institut Mainz, Staudingerweg 18, 55128 Mainz, Germany*
[3]*GSI Helmholtzzentrum für Schwerionenforschung GmbH, Planckstrasse 1, D-64291 Darmstadt, Germany*
[4]*KU Leuven, Instituut voor Kern- en Stralingsfysica, Celestijnenlaan 200D, B-3001 Leuven, Belgium*
[5]*CEST, Skolkovo Institute of Science and Technology, Skolkovo Innovation Center, Nobel Street 3, Moscow 121205, Russia*
[6]*Institute of Problems of Chemical Physics RAS, Chernogolovka, Moscow District 142432, Russia*
[7]*Science Department, Chatham University, Pittsburgh, Pennsylvania 15232, USA*

(Received 6 November 2019; accepted 3 June 2020; published 10 July 2020)

Optical spectroscopy constitutes the historical path to accumulate basic knowledge on the atom and its structure. Former work based on fluorescence and resonance ionization spectroscopy enabled identifying optical spectral lines up to element 102, nobelium. The new challenges faced in this research field are the refractory nature of the heavier elements and the decreasing production yields. A new concept of ion-mobility-assisted laser spectroscopy is proposed to overcome the sensitivity limits of atomic structure investigations persisting in the region of the superheavy elements. The concept offers capabilities of both broadband-level searches and high-resolution hyperfine spectroscopy of synthetic elements beyond nobelium.

DOI: 10.1103/PhysRevLett.125.023002

Chemical elements exhibit atomic emission spectra that are unique and serve as fingerprints. These spectra have long been observed for most of the elements, in the laboratory and even from stars, and have been key ingredients in understanding the cosmic origin of matter [1]. Their exploration to ever higher accuracy in ever heavier elements provides a fertile ground to advance our understanding of the atom's structure, aside from the classic advantage of bridging atomic and nuclear physics [2]. Precise spectroscopic measurements of hyperfine structures and isotope shifts of spectral lines enable the study of single-particle and collective properties of atomic nuclei such as nuclear spins, moments, and mean square charge radii and provide anchor points for nuclear models that are presently applied to pinpoint the "island of stability" of superheavy elements.

A great leap forward in this research field was recently achieved with successful laser spectroscopy of the element nobelium [3]. The experiments provided powerful benchmarks for atomic model calculations [4] and enabled information on the atomic nucleus to be obtained independently from nuclear models [5]. Beyond nobelium, only predictions of the atomic structure exist, which in general are far from sufficient to reliably identify atoms from spectral lines [6].

Experiments remain the only means to discover atomic lines of the heaviest elements and to extend the reference data for *ab initio* calculations. However, the lack of primordial isotopes of these elements combined with the inability of breeding macroscopic amounts in high-flux nuclear reactors renders impossible the traditional way of studying their atomic emission spectra with light from primed arc-discharge tubes [7]. The various techniques currently used to study exotic atoms rely on (i) the atomic structure already being experimentally known, which is not the case for elements beyond nobelium, and (ii) low-energetic atomic beams of the highest quality, from, e.g., Isotope Separator On-Line facilities [8] that are unsuited to superheavy element production.

Superheavy elements are produced, at best, at rates less than one atom per second in heavy-ion induced fusion-evaporation reactions utilizing powerful particle accelerators in conjunction with thin-target production techniques [9]. Recoil separators are used to separate the reaction products from the intense primary beam. The highly charged product ions may have kinetic energies up to multiples of ten MeV and have to first be slowed down to thermal energies for optical spectroscopy. This is best done by stopping them in gas catchers, preferably in inert gases like helium (He) to avoid formation of chemical compounds [10]. The ions are thermalized typically in 1+ and 2+ states [11–14]. Thus far, it has been necessary to neutralize them for resonance ionization spectroscopy (RIS) as in the nobelium studies [3]. In these experiments, electric fields are used to capture the ions on a filament where neutralization takes place. By pulse heating the filament, the accumulated fusion products are released as neutral atoms for subsequent RIS measurements.

Since this release process depends on the surface material and on the physicochemical properties of the sample atoms [15,16], it may result in the emission of unwanted surface ions at elevated temperatures and thus

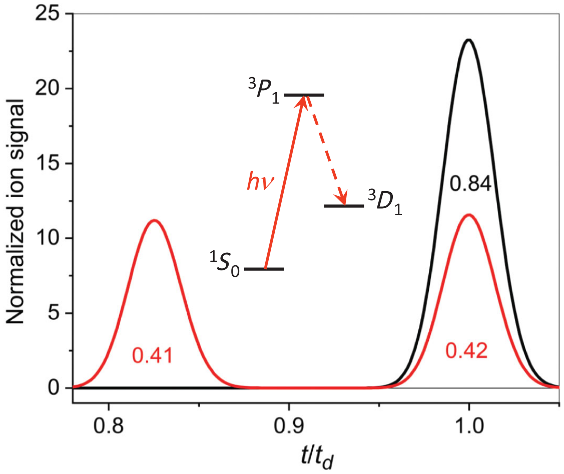

FIG. 1. Lu^+ off-resonance (black curve) and resonant pumping (red curve) signals expected at an effective temperature of metastable ions of 880 K. $L = 4$ cm, $p_0 = 3.5$ mbar He, $T = 100$ K, $E/n_0 = 38$ Td, $t_d = 25$ μs. For the resonant pumping signal, 94% of the ions have an initially occupied $^3D_1$ state. Numbers within the peaks indicate the respective collection efficiencies. (Inset) Simplified scheme for initial optical pumping by laser radiation ($h\nu$) from the $^1S_0$ to $^3D_1$ state.

substantially hamper the applicability of such a RIS method to the refractory transition metals in the region of the superheavy elements. Large efforts are currently undertaken to find ways for a quick neutralization of the product ions in typically large buffer-gas stopping volumes without utilizing catcher filaments, such as exploiting strong beta sources [17], but a solution for RIS-based methods cannot yet be safely predicted. Furthermore, any RIS on superheavy elements would require an extensive search for expected optical transitions within a broad spectral range inferred from atomic model calculations. This in turn necessitates the usage of broadband lasers and aims at simple two-step photoionization schemes [18]. But since ions exhibit ionization potentials that are energetically far above what could be accessible utilizing advanced optical setups, this approach remains limited to neutralized fusion products. Contemporary methods based on fluorescence detection lack sensitivity due to the typically limited solid-angle coverage of detectors in the presence of elevated backgrounds of various origins [19] and thus are not suited for such studies.

In this Letter, an alternate way of optical spectroscopy—termed laser resonance chromatography (LRC)—is proposed for probing the heaviest product ions *in situ*, as extracted from gas catchers behind recoil separators. Its key idea is to detect the products of resonant optical excitations by their characteristic drift time to a particle detector. The method exploits laser excitation of the extracted ions from the ground state to a bright intermediate level (see the inset in Fig. 1). An efficient relaxation to lower-lying metastable states is expected to occur via radiative processes, which is typical for transition metal ions. Since ion mobilities are sensitive to changes in electronic configurations [20,21], such as during optical pumping, guiding these ions through a drift tube enables one to discriminate ions in ground and metastable states by drift times. This effect of electronic state chromatography is well established from ion-mobility spectrometry of many transition metals [22–28]. The time spectra obtained without resonant excitations characterize initial background ions, whereas detecting ions at significantly shorter or longer times signals resonant pumping, which triggers the conversion of the background ions into the metastable ones. LRC has a number of key advantages compared to common optical spectroscopy. Omitting intermediate steps such as neutralization of thermalized fusion products, photoionization of ions, and radiation detection provides a general optical access to elemental cations without sacrificing speed or sensitivity.

The method can be applied to element 103, lawrencium (Lr), which is currently the heaviest element in the focus of RIS experiments [29,30]. As follows from quantitative *ab initio* calculations for Lr^+ [31], pumping the ground state $7s^2\,{}^1S_0$ to the bright $7s7p\,{}^3P_1$ state effectively feeds the lowest $6d7s\,{}^3D_1$ state of a radiative lifetime (25 days) exceeding the half-lives of all known Lr isotopes. The efficiency for optical pumping depends on both the strength of the ground-state transition to the bright intermediate level and on the branching ratios from this level to the lower-lying ground and metastable states. Calculations predict a sizable Einstein coefficient for spontaneous emission of $A_{ki} = 6.36 \times 10^7\ \mathrm{s}^{-1}$ for the ${}^1S_0$-${}^3P_1$ ground-state transition [31]. The intermediate $^3P_1$ level is predicted at $31,540 \pm 389\ \mathrm{cm}^{-1}$ (about 317 nm), which is readily accessible for laser probing. The branching ratio to lower-lying metastable states is expected to be 10% for Lr^+, but it can exceed 50% as in the lighter homologue Lu^+ [32,33]. We implemented a five-level system into a rate equation model to calculate the probability for optical pumping of the metastable ^3D states in Lu^+ and Lr^+ [34]. In the model, we assumed a laser-ion interaction of 10 ns duration every 100 μs at an energy density of the laser radiation of $10\ \mu\mathrm{J/cm}^2$. In addition, we accounted for instantaneous population transfers due to possible ion collisions with residual gas by including the same state-quenching rates as those reported for the isoelectronic neutral barium in He [35]. Starting with a level system in its ground state ($^1S_0$), we obtained a 31.5% probability for optical pumping into the $^3D_1$ state in Lu^+ already for one single pulse exposure. This probability amounts to 7.5% in Lr^+ and reaches values of 94% and 53% after ten pulses for the two ionic species, respectively, which are sufficiently high for the LRC studies.

The mobility K is known for many atomic species in many neutral gases [36]. Macroscopically, it relates the speed v_d of an ion drifting in trace amounts through a dilute gas of pressure p_0 and temperature T to the applied electric field strength E by the equation $v_d = KE$ [37]. Usually, it is

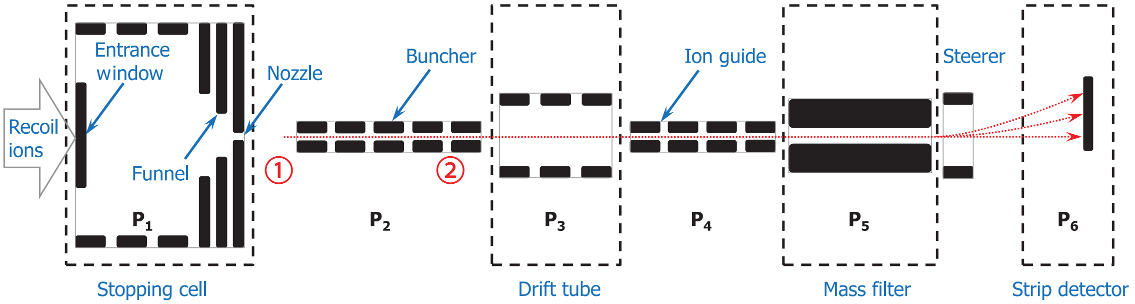

FIG. 2. Schematic view of the LRC setup for on-line experiments. Laser probing of ionic states occurs inside the buncher (position 2) during the level search or in the gas jet (position 1) to enable hyperfine spectroscopy. The dashed lines show potential trajectories of the extracted ions along the apparatus. $P_1 \approx 60$ mbar, $P_2 \approx 5 \times 10^{-2}$ mbar, $P_3 = p_0 < 10$ mbar, $P_4 \approx 10^{-3}$ mbar, $P_5 \approx 10^{-5}$ mbar, and $P_6 \approx 10^{-7}$ mbar. See the text for more details.

reported as the reduced mobility, $K_0 = K(p_0/p_{\mathrm{st}})(T_{\mathrm{st}}/T)$, which implies normalization to the standard temperature ($T_{\mathrm{st}} = 273.15$ K) and pressure ($p_{\mathrm{st}} = 1013.25$ mbar). The mobility can be derived, together with the diffusion coefficients, from the solution of the Boltzmann equation for a steady-state drift of an ion swarm [21,37,38]. Momentum transfer and similar transport cross sections of the ion-neutral collisions are the main parameters that establish the microscopic relation between the transport coefficients, e.g., mobility, and the ion-neutral interaction potential. As the repulsive short-range interaction depends on the electronic configuration, the mobility inevitably inherits this dependence, underpinning the electronic-state-chromatography effect.

Accurate measurements for transition metals [23–25] revealed that the mobility difference may be as large as 33% in the case of different states of Cu^+ ions [25]. Recent systematic measurements across the lanthanides [39] have shown, in agreement with former predictions [40], that the zero-field mobilities of ions with the $4f^n6s$ configuration in He deviate from 19.0 $\mathrm{cm}^2/\mathrm{V\,s}$ within ±3%, whereas for Gd^+ ($4f^75d6s$) and Lu^+ ($4f^{14}6s^2$) ions the deviations approach +9% and −12%, respectively.

To verify the perspectives of discriminating Lr^+ ions in their ground and metastable states, we performed extensive calculations for Lu^+, which has a similar structure of the excited state but, unlike its heavier homologue, has been studied experimentally [39]. The interaction potential for Lu^+ in its ground state with He was computed in Ref. [40] using the single-reference coupled cluster method with singles, doubles, and noniterative correction to triples. The standard mobility in He at room temperature was predicted in these calculations as 16.6 $\mathrm{cm}^2/\mathrm{V\,s}$ and was found to be accurate within 2% when compared with the more recent value of 16.8 ± 0.4 $\mathrm{cm}^2/\mathrm{V\,s}$ reported from mobility measurements at 295 K [39]. A similar approach was followed here to address the interaction of Lu^+ in the $6s5d$ $^3D_1$ metastable state [34]. Configuration interaction methods [41] were implemented to account for spin-orbit coupling. Transport coefficients were computed by solving the Boltzmann equation according to the Gram-Charlier approach [21,38]. Momentum transfer cross sections for the $\Omega = 0^-$ and 1 components of the metastable $^3D_1$ state were averaged to give total cross sections in a way verified recently for the open-shell Gd^+ [42] for which a 1% relative accuracy was achieved. Thus, we expect a similar accuracy for mobilities of Lu^+ in the $^3D_1$ state as for this ion in the ground state.

The calculated transport coefficients indicate that Lu^+ ions in the metastable state drift faster than the ones in the ground state but experience greater diffusion [34]. In addition, the deviation in ion mobility can be as high as 24%.

To better assess the LRC separation capabilities for Lu^+ in the different states, we used the analytical expression derived in Ref. [43] for describing ion swarms drifting in dilute gases [34]. We took an ion swarm starting in the initial state occupation as obtained from the rate equation model after ten laser-pulse exposures and calculated the drift time distributions throughout a drift length L for different pressures, temperatures, and electric fields to gas number densities E/n_0 [34]. Figure 1 shows these distributions for a drift length of 4 cm, $T = 100$ K, $E/n_0 = 38$ Td, with 1 Td (Townsend unit) being equal to 10^{-21} Vm^2, and $p_0 = 3.5$ mbar, which were found to be a good compromise between sufficient time resolution and detection efficiency. In this case, the mean drift time of the ground state ions is 25 μs. Importantly, we show that about 41% of the ions can be collected in the $^3D_1$ state after pumping and drift, despite collisional quenching to the ground state at a rate as measured for barium in He [35] at 880 K. Applying smaller E/n_0 ratios results in less ion heating, which could be necessary to suppress quenching to the ground state at the cost of diffusion losses. Still, a collection efficiency above 28% can be maintained for effective ion temperatures up to 300 K under optimal conditions when longer drift times are envisaged. Also, reducing the initial $^3D_1$ occupation to 53%, as expected from optical pumping in Lr^+, results in sufficiently high collection efficiencies above 16% [34].

From the practical viewpoint, we propose a LRC setup as shown in Fig. 2. It consists of a buffer-gas stopping cell and a detection part allowing for cooling, guiding, selecting, and detecting the ions under investigation. We suggest using helium as a buffer gas in the stopping cell at pressures around 60 mbar, following similar gas catcher concepts devoted to mass measurements [44,45]. The cell incorporates a radio-frequency (rf) funnel and is isolated from the detection part by an extraction nozzle [13,14]. The detection part comprises, sequentially, a rf quadrupole in a bunch-mode operation (called a buncher), a cryogenic drift tube, a second rf quadrupole as an ion guide, a quadrupole mass spectrometer (QMS) for charge-to-mass selection, and a particle detector. Our approach stipulates the use of very short drift tubes filled with He at pressures < 10 mbar in order to suppress unwanted quenching and to pursue the desired resolving power by applying appropriate gas temperatures and E/n_0 ratios. Similar drift tube concepts have been followed in state-specific ion-mobility studies along the third-row transition metals [24,25].

The fusion products provided by recoil separators penetrate the stopping cell through an entrance foil and thermalize mostly as ions in high purity helium [46]. Adding small quantities of chemically inert gases like krypton or xenon of relatively low ionization thresholds into the buffer gas helps to shift the ion charge states to 1+ without significant ion losses. The ion manipulation by electric dc and rf fields enables a fast and efficient extraction of the fusion products within the emerging buffer gas that flows continuously through the nozzle. Using a laser beam of tunable wavelengths from a pulsed laser system [47], one can search for ground-state transitions of the sample ions trapped in the buncher [48] (position 2 in Fig. 2) at background pressures $\leq 5 \times 10^{-2}$ mbar. The expected Doppler and power broadening of the spectral lines enable a relatively quick and efficient search for optical resonances. The singly charged ions will then be in either the ground- or the metastable-state configuration during their transport downstream to the drift tube. Gas cooling inside the buncher will facilitate the injection into the drift tube. Bunched ions passing the drift tube, the ion guide, and the QMS will be detected with, e.g., a Channeltron detector placed in a high-vacuum section. The time differences between buncher timing and detector-signal time stamps describe arrival time distributions, which will be monitored for long time periods during the level search. At constant background conditions, a high sensitivity for resonance detection can be reached because successful laser excitations trigger optical pumping, change the ratio of metastable ions to ground-state ions of distinct mobilities, and thus cause a change in the time distributions [34]. On establishing a ground-state transition, like the predicted ${}^1S_0$-${}^3P_1$ transition in Lr$^+$, much more precise LRC measurements can be performed by probing the ions transported in the cold supersonic gas jet of low density [29] formed in front of the nozzle (position 1 in Fig. 2). In the case of elevated background ions, an increased sensitivity of the setup can be achieved by a synchronized steering of the mass-selected ions along a position-sensitive Si-strip detector (SSD). Since the radionuclides of interest are α emitters, the drift time information will then be imprinted in the position of the α-activity hot spots on the Si detector (Fig. 2). This way of ion detection allows (i) a zoom in the time line when the steering process is initiated at the expected arrival time of the ions and (ii) a nearly background-free ion detection at rates down to one count per hour or even less due to the fingerprint α-decay detection.

TABLE I. Expected partial and overall efficiencies for LRC on Lu$^+$.

Type	Efficiency (%)
Stopping and extraction	10–33
Fraction of 1+ ions	50–70
Initial ground-state occupation	50
Buncher transmission	90
Lu$^+$ (${}^3D_1$) collection from drift tube [a]	28–41
Ion guide transmission	90
QMS transmission	90
Ion detection[b]	40–100
In total	0.2–3.5

[a] Considers optical pumping and signal losses due to transverse diffusion and quenching [34].

[b] Taken 100% when using a Channeltron and about 40% when using a position-sensitive SSD for α-decay detection.

The stopping and extraction of the fusion products can be as efficient as 10% at room temperature [49]. An increased efficiency of about 33% can be achieved if a cryogenic stopping cell is used [14]. We expect 50% to 70% of the extracted products to be singly charged monatomic ions, out of which we expect 50% at least to be in their ground state. Here we give a rather conservative estimate for this ion fraction, as elevated pressures inside the stopping cell promote fast relaxation processes during a comparably slow extraction. In addition, we expect a transmission through the rf quadrupole structures to be about 80% for light ions [17], while a slightly higher transmission efficiency (90%) can be achieved for the heaviest elements. We do not expect losses due to space charge effects to play a significant role since these usually alter the transmission for bunches containing more than 10^4 ions [17], which will not be the case for elements beyond nobelium. The transmission of the ions through the QMS amounts to 90% at a moderate mass resolution [50]. Table I summarizes the expected partial efficiencies for the LRC method. Taking the collection efficiency of the drift tube into account, one ends up with an overall efficiency of the apparatus of 0.2%–3.5% for Lu$^+$. Similar values should be reachable for Lr$^+$ and other heavier elements. Although small, these values are at least 2 orders of magnitude larger than what can be achieved for common fluorescence-based spectroscopy and similar to those recently reported for resonance ionization spectroscopy across the actinides [3,29].

In summary, LRC should be a sensitive and versatile technique of optical spectroscopy that will enable both broadband-level searches and narrow-band hyperfine spectroscopy on elements thus far inaccessible in the periodic table beyond nobelium. Atomic model calculations predict a strong $^1S_0$-$^3P_1$ ground-state transition in Lr^+ at about 317 nm, which is envisaged for future LRC investigations [31]. In addition, the method can be used to explore the atomic structure of the superheavy elements (rutherfordium and dubnium) of refractory nature that are available only in minute production quantities [49,51].

Other ionic species like triply charged thorium (Th^{3+}) [52–54] should be within reach of the LRC method as well. Th^{3+} exhibits a long-lived metastable atomic state for optical probing as well as suitable laser cooling transitions [55] making it an ideal candidate for the realization of a future frequency standard based on the nuclear isomer $^{229m}\mathrm{Th}$ [56]. Moreover, an axial injection of a continuous-wave laser beam through the drift tube makes the method more universal because average drift times of ions in ground and excited states result whenever the resonance conditions are fulfilled and the respective mobilities are distinct. Finally, the ability to optically pump ions in a controlled way has the potential to make further optical transitions accessible and to provide state-purified cations for chemistry experiments [26] and benchmark data for state-of-the-art *ab initio* calculations.

We thank M. Verlinde, R. Ferrer, S. Raeder, F. Schneider, T. Murböck, J. Berengut, A. Borschevsky, P. Van Duppen, M. Block, H. Backe, and H.-J. Kluge for the fruitful discussions on the LRC concept. A. A. B. acknowledges the support of the Russian Foundation for Basic Research (Project No. 19-03-00144). This project has received funding from the European Research Council (ERC) under the European Union's Horizon 2020 research and innovation programme (Grant Agreement No. 819957).

---

[*] mlaatiao@uni-mainz.de

[1] A. Frebel and C. B. Timothy, The formation of the heaviest elements, Phys. Today **71**, No. 1, 30 (2018).

[2] K. Blaum, J. Dilling, and W. Nörtershäuser, Precision atomic physics techniques for nuclear physics with radioactive beams, Phys. Scr. **T152**, 014017 (2013).

[3] M. Laatiaoui *et al.*, Atom-at-a-time laser resonance ionization spectroscopy of nobelium, Nature (London) **538**, 495 (2016).

[4] P. Chhetri *et al.*, Precision Measurement of the First Ionization Potential of Nobelium, Phys. Rev. Lett. **120**, 263003 (2018).

[5] S. Raeder *et al.*, Probing Sizes and Shapes of Nobelium Isotopes by Laser Spectroscopy, Phys. Rev. Lett. **120**, 232503 (2018).

[6] V. A. Dzuba, V. V. Flambaum, and J. K. Webb, Isotope shift and search for metastable superheavy elements in astrophysical data, Phys. Rev. A **95**, 062515 (2017).

[7] E. F. Worden *et al.*, Spectra and electronic structures of free actinide atoms and ions, in *The Chemistry of the Actinide and Trans-Actinide Elements*, edited by J. Fuger, L. R. Morss, and M. Edelstein (Springer, Dordrecht, 2008), Vol. 3.

[8] P. Van Duppen, Isotope separation on line and post acceleration, in *The Euroschool Lectures on Physics with Exotic Beams, Vol. II*, Lecture Notes in Physics Vol. 700, edited by J. Al-Khalili and E. Roeckl (Springer, Berlin, 2006).

[9] M. Schädel, The chemistry of transactinide elements—Experimental achievements and perspectives, J. Nucl. Radiochem. Sci. **3**, 113 (2002).

[10] H. Backe, W. Lauth, M. Block, and M. Laatiaoui, Prospects for laser spectroscopy, ion chemistry and mobility measurements of superheavy elements in buffer-gas traps, Nucl. Phys. **A944**, 492 (2015).

[11] C. Droese *et al.*, High-precision mass measurements of $^{203-207}\mathrm{Rn}$ and $^{213}\mathrm{Ra}$ with SHIPTRAP, Eur. Phys. J. A **49**, 13 (2013).

[12] F. Lautenschläger *et al.*, Developments for resonance ionization laser spectroscopy of the heaviest elements at SHIP, Nucl. Instrum. Methods Phys. Res., Sect. B **383**, 115 (2016).

[13] C. Droese *et al.*, The cryogenic gas stopping cell of SHIPTRAP, Nucl. Instrum. Methods Phys. Res., Sect. B **338**, 126 (2014).

[14] O. Kaleja *et al.*, The performance of the cryogenic buffer-gas stopping cell of SHIPTRAP, Nucl. Instrum. Methods Phys. Res., Sect. B **463**, 280 (2020).

[15] M. Laatiaoui, H. Backe, M. Block, F.-P. Heßberger, P. Kunz, F. Lautenschläger, W. Lauth, M. Sewtz, and T. Walther, On laser spectroscopy of the element nobelium ($Z = 102$), Eur. Phys. J. D **68**, 71 (2014).

[16] T. Murböck, S. Raeder, P. Chhetri, K. Diaz, M. Laatiaoui, F. Giacoppo, and M. Block, Filament studies for laser spectroscopy on lawrencium, Hyperfine Interact. **241**, 35 (2020).

[17] R. Ferrer *et al.*, In gas laser ionization and spectroscopy experiments at the Superconducting Separator Spectrometer (S^3): Conceptual studies and preliminary design, Nucl. Instrum. Methods Phys. Res., Sect. B **317**, 570 (2013).

[18] V. Letokhov, *Laser Photoionization Spectroscopy* (Academic Press, New York, 1987).

[19] P. Campbell, I. D. Moore, and M. R. Pearson, Laser spectroscopy for nuclear structure physics, Prog. Part. Nucl. Phys. **86**, 127 (2016).

[20] M. Laatiaoui, H. Backe, D. Habs, P. Kunz, W. Lauth, and M. Sewtz, Low-field mobilities of rare-earth metals, Eur. Phys. J. D **66**, 232 (2012).

[21] L. A. Viehland, *Gaseous Ion Mobility, Diffusion, and Reaction* (Springer Nature, Cham, Switzerland, 2018).

[22] P. R. Kemper and M. T. Bowers, Electronic-state chromatography: Application to first-row transition-metal ions, J. Phys. Chem. **95**, 5134 (1991).

[23] W. S. Taylor, E. M. Spicer, and D. F. Barnas, Metastable metal ion production in sputtering dc glow discharge plasmas: Characterization by electronic state chromatography, J. Phys. Chem. A **103**, 643 (1999).

[24] C. Iceman, C. Rue, R. M. Moision, B. K. Chatterjee, and P. B. Armentrout, Ion mobility studies of electronically excited states of atomic transition metal cations: Development of an ion mobility source for guided ion beam experiments, J. Am. Soc. Mass Spectrom. **18**, 1196 (2007).

[25] Y. Ibrahim, E. Alsharaeh, R. Mabrouki, P. Momoh, E. Xie, and M. S. El-Shall, Ion mobility of ground and excited states of laser-generated transition metal cations, J. Phys. Chem. A **112**, 1112 (2008).

[26] P. B. Armentrout, Electronic state chromatography, in *Ion Mobility Spectrometry-Mass Spectrometry*, edited by S. Trimpin and C. L. Wilkins (CRC Press, Boca Raton, 2011).

[27] M. J. Manard and P. R. Kemper, Ion mobility mass spectrometry: The design of a new high-resolution ion mobility instrument with applications toward electronic-state characterization of first-row transition metal cations, Int. J. Mass Spectrom. **402**, 1 (2016).

[28] M. J. Manard and P. R. Kemper, Characterizing the electronic states of the second-row transition metal cations using high-resolution ion mobility mass spectrometry, Int. J. Mass Spectrom. **407**, 69 (2016).

[29] R. Ferrer *et al.*, Towards high-resolution laser ionization spectroscopy of the heaviest elements in supersonic gas jet expansion, Nat. Commun. **8**, 14520 (2017).

[30] M. Laatiaoui and S. Raeder, Laser spectroscopy of the heaviest elements: One atom at a time, Nucl. Phys. News **29**, 21 (2019).

[31] E. V. Kahl, J. C. Berengut, M. Laatiaoui, E. Eliav, and A. Borschevsky, High-precision *ab initio* calculations of the spectrum of Lr^+, Phys. Rev. A **100**, 062505 (2019).

[32] P. Quinet, P. Palmeri, E. Biémont, M. M. McCurdy, G. Rieger, E. H. Pinnington, M. E. Wickliffe, and J. E. Lawler, Experimental and theoretical radiative lifetimes, branching fractions and oscillator strengths in Lu II, Mon. Not. R. Astron. Soc. **307**, 934 (1999).

[33] E. Paez, K. J. Arnold, E. Hajiyev, S. G. Porsev, V. A. Dzuba, U. I. Safronova, M. S. Safronova, and M. D. Barrett, Atomic properties of Lu^+, Phys. Rev. A **93**, 042112 (2016).

[34] M. Laatiaoui, A. Buchachenko, and L. A. Viehland, companion paper, Exploiting transport properties for the detection of optical pumping in heavy ions, Phys. Rev. A **102**, 013106 (2020).

[35] J. Brust and A. C. Gallagher, Excitation transfer in barium by collisions with noble gases, Phys. Rev. A **52**, 2120 (1995).

[36] See http://www.lxcat.net for the Plasma Data Exchange Project (2020).

[37] E. Mason and E. McDaniel, *Transport Properties of Ions in Gases* (John Wiley & Sons, New York, 1988).

[38] L. A. Viehland, Velocity distribution functions and transport coefficients of atomic ions in atomic gases by a Gram-Charlier approach, Chem. Phys. **179**, 71 (1994).

[39] M. J. Manard and P. R. Kemper, Reduced mobilities of lanthanide cations measured using high-resolution ion mobility mass spectrometry with comparisons between experiment and theory, Int. J. Mass Spectrom. **412**, 14 (2017).

[40] A. A. Buchachenko and L. A. Viehland, Mobility of singly-charged lanthanide cations in rare gases: Theoretical assessment of the state specificity, J. Chem. Phys. **140**, 114309 (2014).

[41] A. Berning, M. Schweizer, H.-J. Werner, P. J. Knowles, and P. Palmieri, Spin-orbit matrix elements for internally contracted multireference configuration interaction wavefunctions, Mol. Phys. **98**, 1823 (2000).

[42] A. A. Buchachenko and L. A. Viehland, *Ab initio* study of the mobility of Gd^+ ions in He and Ar gases, Int. J. Mass Spectrom. **443**, 86 (2019).

[43] J. T. Moseley, I. R. Gatland, D. W. Martin, and E. W. McDaniel, Measurement of transport properties of ions in gases: Results for K^+ ions in N_2, Phys. Rev. **178**, 234 (1969).

[44] J. Neumayr *et al.*, The ion-catcher device for SHIPTRAP, Nucl. Instrum. Methods Phys. Res., Sect. B **244**, 489 (2006).

[45] M. Block *et al.*, Direct mass measurements above uranium bridge the gap to the island of stability, Nature (London) **463**, 785 (2010).

[46] E. M. Ramirez *et al.*, Direct mapping of nuclear shell effects in the heaviest elements, Science **337**, 1207 (2012).

[47] Y. Kudryavtsev, R. Ferrer, M. Huyse, P. Van den Bergh, and P. Van Duppen, The in-gas-jet laser ion source: Resonance ionization spectroscopy of radioactive atoms in supersonic gas jets, Nucl. Instrum. Methods Phys. Res., Sect. B **297**, 7 (2013).

[48] P. E. Toschek and W. Neuhauser, Single ions for Doppler-free spectroscopy, Phys. Blätter **36**, 198 (1980).

[49] M. Block, Direct mass measurements of the heaviest elements with Penning traps, Nucl. Phys. **A944**, 471 (2015).

[50] E. Haettner, W. R. Plaß, U. Czok, T. Dickel, H. Geissel, W. Kinsel, M. Petrick, T. Schäfer, and C. Scheidenberger, A versatile triple radiofrequency quadrupole system for cooling, mass separation and bunching of exotic nuclei, Nucl. Instrum. Methods Phys. Res., Sect. A **880**, 138 (2018).

[51] D. Ackermann, Nuclear spectroscopy in nuclei with $Z \geq 110$, Nucl. Phys. **A944**, 376 (2015).

[52] C. J. Campbell, A. G. Radnaev, and A. Kuzmich, Wigner Crystals of $^{229}\mathrm{Th}$ for Optical Excitation of the Nuclear Isomer, Phys. Rev. Lett. **106**, 223001 (2011).

[53] L. von der Wense, B. Seiferle,, M. Laatiaoui, and P. G. Thirolf, The extraction of $^{229}\mathrm{Th}^{3+}$ from a buffer-gas stopping cell, Nucl. Instrum. Methods Phys. Res., Sect. B **376**, 260 (2016).

[54] L. von der Wense *et al.*, Direct detection of the $^{229}\mathrm{Th}$ nuclear clock transition, Nature (London) **533**, 47 (2016).

[55] U. I. Safronova, W. R. Johnson, and M. S. Safronova, Excitation energies, polarizabilities, multipole transition rates, and lifetimes in Th IV, Phys. Rev. A **74**, 042511 (2006).

[56] B. Seiferle *et al.*, Energy of the $^{229}\mathrm{Th}$ nuclear clock transition, Nature (London) **573**, 243 (2019).